Chapter 3
Photon Transfer Noise Sources

When photons strike a detector, interactions immediately produce a signal variance or *noise* from pixel-to-pixel. This chapter introduces four fundamental noise sources important to PT work. The first two sources, *signal shot noise* and *Fano noise*, are related to photon interaction. The third noise source, *fixed pattern noise*, is associated with pixel-to-pixel sensitivity nonuniformity. The fourth source, *read noise*, encompasses all other noise sources that are not dependent on signal strength. Shot noise increases by the square root of signal, whereas FPN increases proportionally with signal. Fano noise increases by the square root of photon energy (or quantum yield).

3.1 Photon Shot Noise

Signal shot noise is fundamentally connected to the way photons spatially arrive on a detector. For example, Fig. 3.1 shows a Monte Carlo simulation where 200 photons are randomly interacting with a 20×20 pixel region. As can be seen, the number of photon interactions varies from zero to four interactions per pixel. The standard deviation (or rms) for the number of interactions per pixel is called *photon shot noise*.

Photon shot noise—a spatially and temporally random phenomenon described by Bose-Einstein statistics—is expressed by

$$\sigma_{\mathrm{SHOT}}(P_{\mathrm{I}})^2 = P_{\mathrm{I}} \frac{e^{hc/\lambda kT}}{e^{hc/\lambda kT} - 1}, \tag{3.1}$$

where $\sigma_{\mathrm{SHOT}}(P_{\mathrm{I}})^2$ is the interacting photon shot noise variance, h is Planck's constant (6.626×10^{-34} J-s), λ is the photon wavelength (cm), k is Boltzmann's constant (1.38×10^{-23} J/K), c is the speed of light (2.99×10^{8} m/sec), and T is absolute temperature (K).[2–4]

Figure 3.2 plots Eq. (3.1) as a function of wavelength (μm) and the temperature of the semiconductor. For wavelengths greater than 10 μm, photons couple with phonons (i.e., lattice vibrations in a solid) that increase the shot noise. As the operating temperature is reduced, the semiconductor produces less coupling action and variance as seen in the plot. However, for silicon detectors this phenomenon is not observed since the photoelectric effect for wavelengths >1 μm can not take

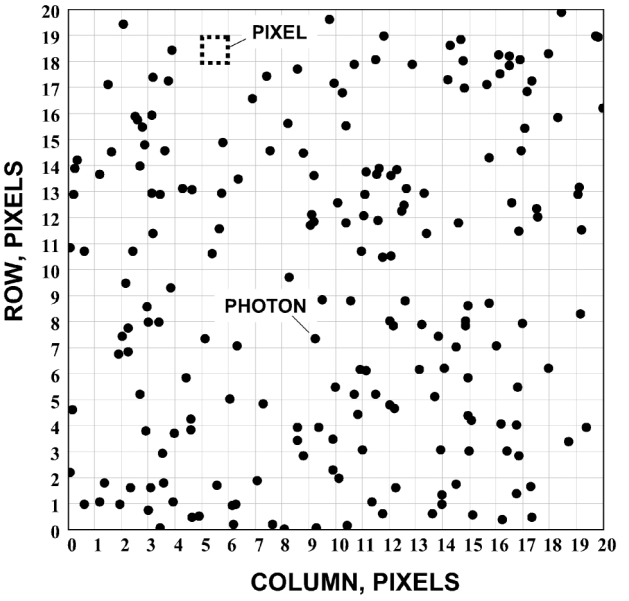

Figure 3.1 Monte Carlo simulation showing photons interacting with pixels.

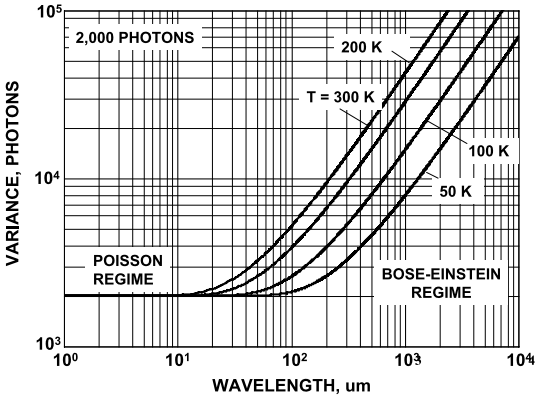

Figure 3.2 Photon shot noise variance as a function of wavelength.

place. Assuming that $hc/\lambda \gg kT$, Eq. (3.1) reduces to the familiar shot noise relation characteristic of visible imagers as

$$\sigma_{\mathrm{SHOT}}(P_{\mathrm{I}}) = P_{\mathrm{I}}^{1/2}. \tag{3.2}$$

Photon shot noise is described by the classical Poisson probability distribution,

$$p_i = \frac{P_{\mathrm{I}}^i}{i!} e^{-P_{\mathrm{I}}}, \tag{3.3}$$

where p_i is the probability that there are i interactions per pixel.

Example 3.1

Find the probability that 0, 1, 2, and 3 photons interact with a pixel, assuming an average of 1 interacting photon per pixel.

Solution:
From Eq. (3.3):

$$p_0 = \frac{1^0}{0!}e^{-1} = 0.368 \quad \text{0 photon interactions}$$

$$p_1 = \frac{1^1}{1!}e^{-1} = 0.368 \quad \text{1 photon interaction}$$

$$p_2 = \frac{1^2}{2!}e^{-1} = 0.184 \quad \text{2 photon interactions}$$

$$p_3 = \frac{1^3}{3!}e^{-1} = 0.0613 \quad \text{3 photon interactions}$$

Figure 3.3 shows results from a random number generator governed by Poisson statistics. The histogram plots occurrences as a function of interacting photons per pixel, assuming 90,000 pixels and 90,000 interacting photons (i.e., $P_{\mathrm{I}} = 1$). The resultant distribution follows the Poisson formula given by Eq. (3.3). For example, 33,200 pixels have one photon interaction, whereas 33,070 pixels show no interactions. The results are expanded and plotted in Fig. 3.4 on a log curve that shows six pixels with seven events.

Figure 3.3 also shows a Gaussian curve to fit data for Example 3.1 that follows

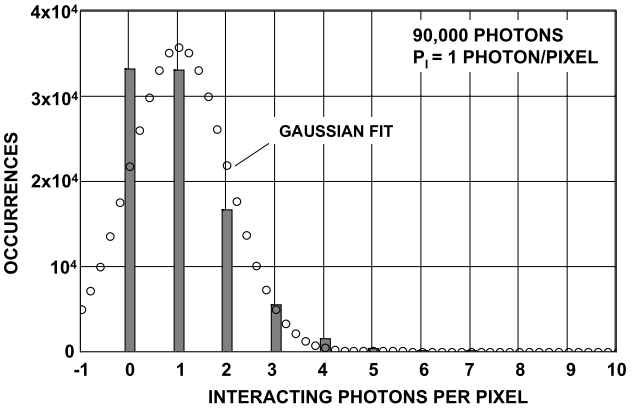

Figure 3.3 Interacting-photons-per-pixel histogram for Fig. 3.1 assuming 1 photon/pixel average.

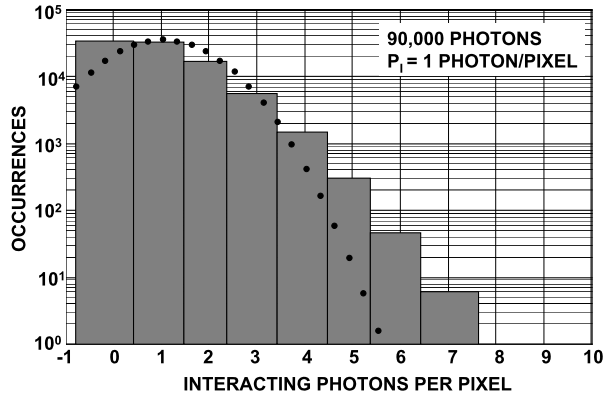

Figure 3.4 Logarithmic histogram for Fig. 3.3.

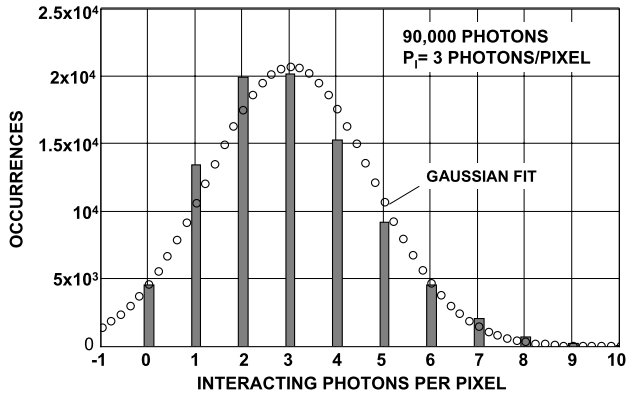

Figure 3.5 Interacting-photons-per-pixel histogram assuming 3 photons/pixel average.

the relation

$$p_i = \frac{1}{(2\pi)^{1/2}\sigma_{\mathrm{PI}}} e^{-(i-P_{\mathrm{I}})^2/2\sigma_{\mathrm{PI}}^2}. \tag{3.4}$$

A Gaussian distribution approximates a Poisson distribution when the number of interacting photons per pixel is large. For example, Fig. 3.5 is a histogram plot that assumes $P_{\mathrm{I}} = 3$, which exhibits a better fit to the Poisson distribution. Figure 3.6 is a histogram for $P_{\mathrm{I}} = 20$ and shows a near-perfect normal distribution.

3.2 Signal Shot Noise

The signal shot noise generated by interacting photons is given by

$$\sigma_{\mathrm{SHOT}} = \eta_{\mathrm{i}}(P_{\mathrm{I}})^{1/2}, \tag{3.5}$$

where σ_{SHOT} is the signal shot noise (rms e^-). Substituting Eq. (2.8) into Eq. (3.5) yields

$$\sigma_{\mathrm{SHOT}} = (\eta_{\mathrm{i}} S)^{1/2}. \tag{3.6}$$

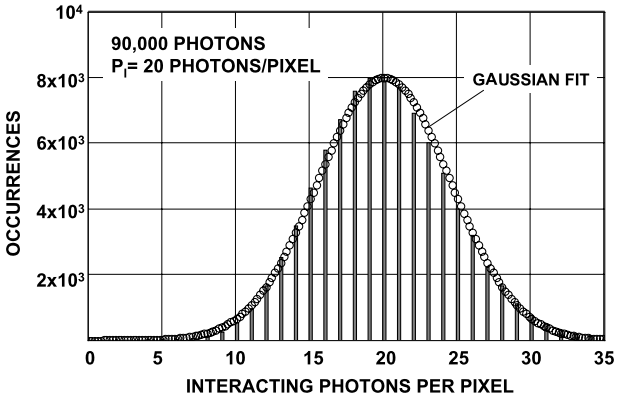

Figure 3.6 Interacting-photon-per-pixel histogram assuming 20 photons/pixel average.

Equation (3.6) is used extensively throughout this book. The relation will be verified through simulation in Figs. 3.9–3.11.

Example 3.2

Assume from Example 3.1 that each interacting photon generates an electron. Add random noise to the response histogram shown in Fig. 3.3 to produce histograms for the following noise levels: 0.1, 0.2, 0.3, 0.4, and 0.5 e^- rms.

Solution:
Figure 3.7 shows the desired histograms. Note that the noise degrades the resolution between electron peaks. Although some CCD and CMOS imagers exhibit read noise levels slightly less than 1 e^-, the noise level is still too high to resolve single-photon interactions. Is it coincidental that the detector's noise level is just shy of doing this?

3.3 Fano Noise

If all the energy of an interacting photon was spent in the production of electron-hole (e-h) pairs, then there would be no variation in the number of e-h pairs produced. On the other hand, if the energy was partitioned between breaking covalent bonds and lattice vibrations, or if phonon production was uncorrelated, Poisson statistics would apply. But neither is the case in nature. The variance in multiple electron-hole charge generation, called *Fano noise*, is empirically described by

$$\sigma_{\mathrm{FN}} = (F_{\mathrm{F}}\eta_{\mathrm{i}})^{1/2} = \left(F_{\mathrm{F}}\frac{h_\nu}{E_{\text{e-h}}}\right)^{1/2}, \tag{3.7}$$

where σ_{FN} is the Fano noise (e^- rms), and F_{F} is referred to as the *Fano factor*, which is defined by the variance in the number of electrons generated divided by

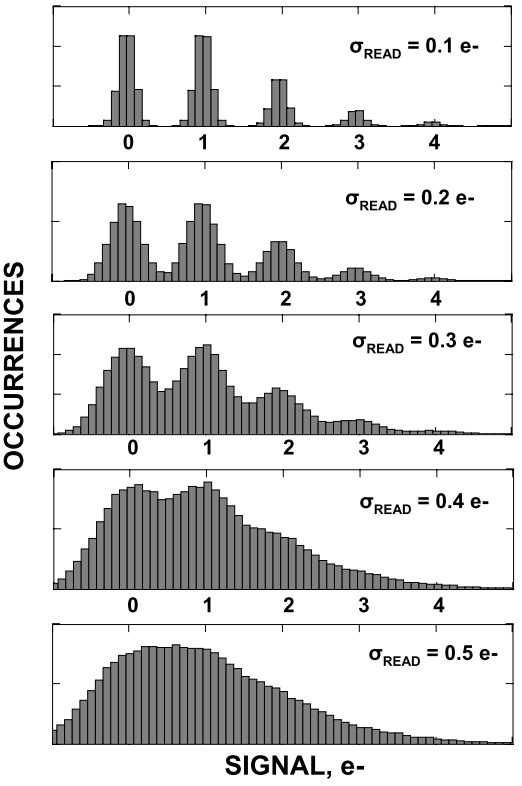

Figure 3.7 Histograms showing influence of different read noise levels on Fig. 3.3.

the average number of electrons generated per interacting photon. The Fano factor is approximately 0.1 for silicon and is applicable for photon energies greater than 10 eV.[1] Figure 3.8 plots Fano noise as a function of photon energy and wavelength. Note that Fano noise becomes appreciable in the soft x-ray regime (i.e., when greater than the read noise floor of 1 e^- rms). Ultra-low read noise CCD and CMOS imagers and cameras are Fano noise-limited through out the x-ray spectrum (and are referred to as such).

Example 3.3

Determine the Fano noise, assuming a quantum yield of 1620 e^- per interacting photon ($h_\nu = 5.9$ keV).

Solution:
From Eq. (3.7),

$$\sigma_{\mathrm{FN}} = (0.1 \times 1620)^{1/2} = 12.7\ \mathrm{e}^-.$$

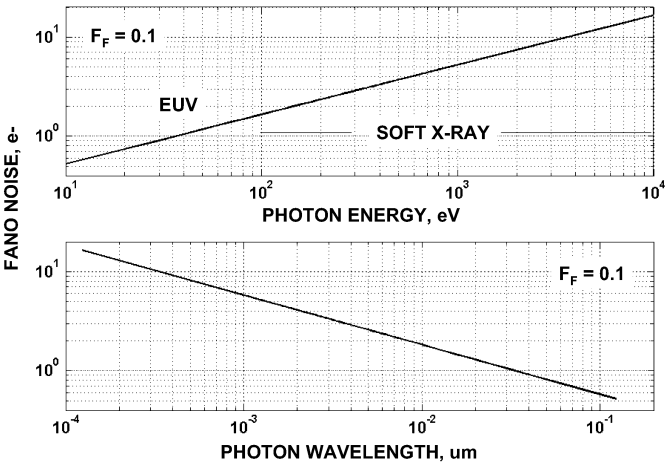

Figure 3.8 Fano noise as a function of photon energy and wavelength.

Figure 3.9 presents a simulation experiment where 90,000 pixels are exposed to an average photon flux of three interacting photons/pixel with $\eta_{\mathrm{i}} = 10\ \mathrm{e}^{-}$/interacting photons. Note that the signal peaks that define the Poisson envelope are separated by 10 e^{-} at locations given by

$$S_{\mathrm{PEAK}} = N_{\mathrm{P}}\eta_{\mathrm{i}}, \tag{3.8}$$

where S_{PEAK} is the signal charge peak level, and N_{P} is the number of multiple photon interactions per pixel that take place. For example, $N_{\mathrm{P}} = 4$ produces a signal peak at 40 e^{-}.

The corresponding standard deviation caused by Fano noise about each signal peak is given by

$$\sigma_{\mathrm{FN\_PEAK}} = (N_{\mathrm{P}}F_{\mathrm{F}}\eta_{\mathrm{i}})^{1/2}. \tag{3.9}$$

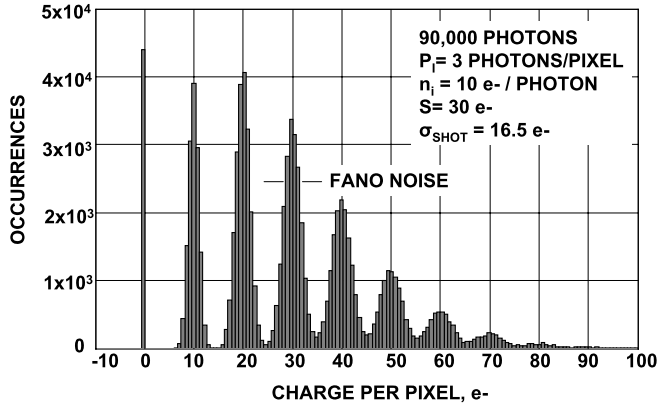

Figure 3.9 Charge-generated-per-pixel histogram with Fano noise present ($n_{\mathrm{i}} = 10\ \mathrm{e}^{-}$/ photon, $P_{\mathrm{I}} = 3$ photons/pixel).

Note that the noise about each peak increases with N_{P} because the Fano noise for multiple pixel-photon interactions is added in quadrature by $(N_{\mathrm{P}})^{1/2}$. This broadening effect is seen in Fig. 3.9, where the separation between signal peaks is less pronounced. Figure 3.10 shows a similar histogram where the average photon flux rate is increased from three to 10 interacting photons/pixel. Note that the signal peaks are unresolved for large N_{P} because of Fano noise. Figure 3.11 shows how the resolution improves when the quantum yield is increased from 10 to 30 electrons/interacting photon.

When signal shot noise and Fano noise are added in quadrature, the net noise is

$$\sigma_{\mathrm{SHOT+FN}} = (\sigma^2_{\mathrm{SHOT}} + \sigma^2_{\mathrm{FN}})^{1/2}. \tag{3.10}$$

Substituting Eqs. (3.6) and (3.7) into Eq. (3.10) yields

$$\sigma_{\mathrm{SHOT+FN}} = \left(\eta_{\mathrm{i}}(S + F_{\mathrm{F}})\right)^{1/2}. \tag{3.11}$$

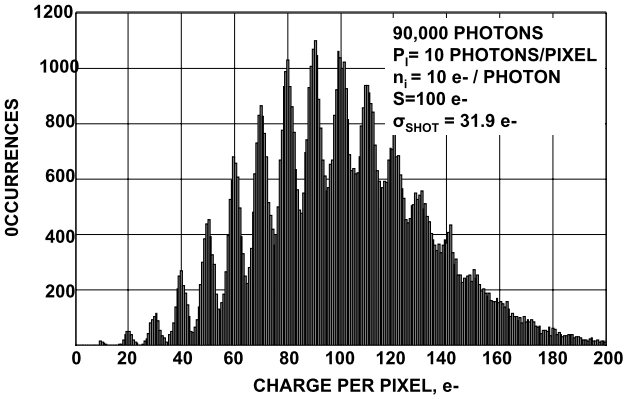

Figure 3.10 Charge-generated-per-pixel histogram with Fano noise ($n_{\mathrm{i}} = 10$ e$^-$/photon, $P_{\mathrm{I}} = 10$ photons/pixel).

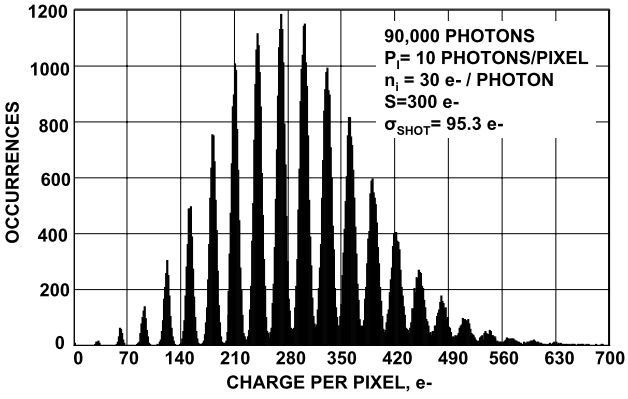

Figure 3.11 Charge-generated-per-pixel histogram with Fano noise ($n_{\mathrm{i}} = 30$ e$^-$/photon, $P_{\mathrm{I}} = 10$ photons/pixel).

Note that relative to signal shot noise, Fano noise is only important when the number of photon interactions per pixel is very small (i.e., when the average signal is small). Figure 3.12 shows a PTC plot of σ_{SHOT} and $\sigma_{\mathrm{SHOT+FN}}$ as a function of signal and different quantum yields. Fano noise is only significant in the plots when $S < 1\,\mathrm{e}^-$. This condition takes place for single photon detection x-ray applications.

Example 3.4

Determine the signal shot noise and Fano noise for the histograms shown in Figs. 3.9–3.11.

Solution:
From Eqs. (3.6) and (3.7),
Figure 3.9 ($\eta_{\mathrm{i}} = 10$, $P_{\mathrm{I}} = 3$)

$$\begin{aligned} \sigma_{\mathrm{SHOT}} &= 10(3)^{1/2} = 17.32\,\mathrm{e}^- \\ \sigma_{\mathrm{FN}} &= (0.1 \times 10)^{1/2} = 1\,\mathrm{e}^- \end{aligned}$$

Figure 3.10 ($\eta_{\mathrm{i}} = 10$, $P_{\mathrm{I}} = 10$)

$$\begin{aligned} \sigma_{\mathrm{SHOT}} &= 10(10)^{1/2} = 31.63\,\mathrm{e}^- \\ \sigma_{\mathrm{FN}} &= (0.1 \times 10)^{1/2} = 1\,\mathrm{e}^- \end{aligned}$$

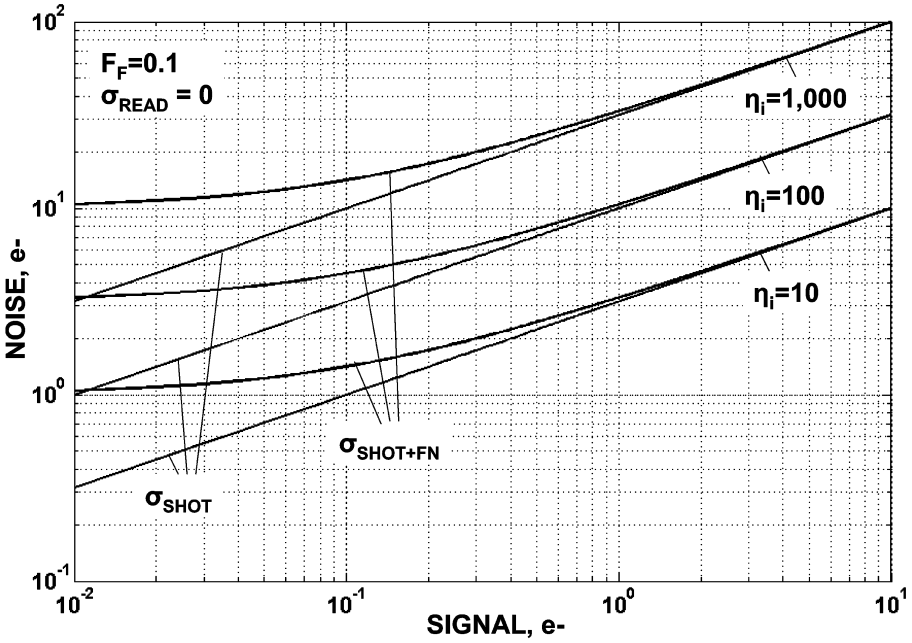

Figure 3.12 PTCs showing Fano noise dominating shot noise for small average signals.

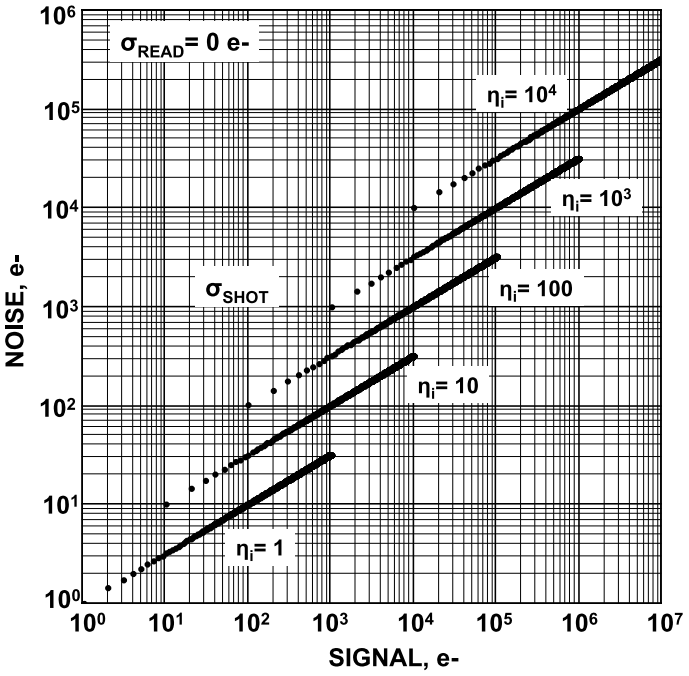

Figure 3.13 Shot noise versus signal PTCs for different quantum yields.

Figure 3.11 ($\eta_{\rm i} = 30$, $P_{\rm I} = 10$)

$$\begin{aligned} \sigma_{\rm SHOT} &= 30(10)^{1/2} = 95\ {\rm e}^- \\ \sigma_{\rm FN} &= (0.1 \times 30)^{1/2} = 1.732\ {\rm e}^- \end{aligned}$$

Figure 3.13 plots $\sigma_{\rm SHOT}$ as a function of S and different $\eta_{\rm i}$. Note that for a given signal level, the signal shot noise increases by the square root of quantum yield [i.e., Eq. (3.6)].

3.4 Fixed Pattern Noise

After the photoelectric effect takes place, the pixels collect the photoelectrons generated. The charge collection process is not perfect because some pixels collect charge more efficiently than others, resulting in pixel-to-pixel sensitivity differences. The effect generates FPN in an image.[1] This noise is called "fixed" because it is not random—it is spatially the same pattern from image to image.

FPN is defined by the relation

$$\sigma_{\rm FPN} = P_{\rm N} S, \tag{3.12}$$

where $\sigma_{\rm FPN}$ is the FPN (rms e^-), and $P_{\rm N}$ is the FPN quality factor, which is approximately 0.01 (1%) for CCD and CMOS sensors.

P_{N} is one of the first data products produced by a PTC (refer to Chapter 5). It is measured by the ratio of rms noise to the mean signal for a uniform light stimulus. For example, a 1% FPN implies that the rms noise is 1% of the mean signal level.

Unlike shot noise, which varies as the square root of signal [i.e., Eq. (3.6)], FPN is proportional to signal. It is for this reason that FPN for visible and near-IR applications will dominate signal shot noise over most of a sensor's dynamic range. This characteristic will be very important to signal-to-noise performance discussions in Chapter 10.

Example 3.5

Compare signal shot noise and FPN for a signal level of 2×10^5 e^-. Assume $\eta_{\mathrm{i}} = 1$ and $P_{\mathrm{N}} = 0.05$.

Solution:
From Eq. (3.6), the shot noise is

$$\sigma_{\mathrm{SHOT}} = (2 \times 10^5)^{1/2} = 447\ \mathrm{e}^-.$$

From Eq. (3.12), the FPN is

$$\sigma_{\mathrm{FPN}} = (2 \times 10^5) \times 0.05 = 10{,}000\ \mathrm{e}^-.$$

Figure 3.14 presents a sinusoidal image that possesses maximum and minimum signal excursions of 200,000 and 0 e^-, respectively, assuming $P_{\mathrm{N}} = 5\%$. The images demonstrate the signal-to-noise difference when FPN dominates.

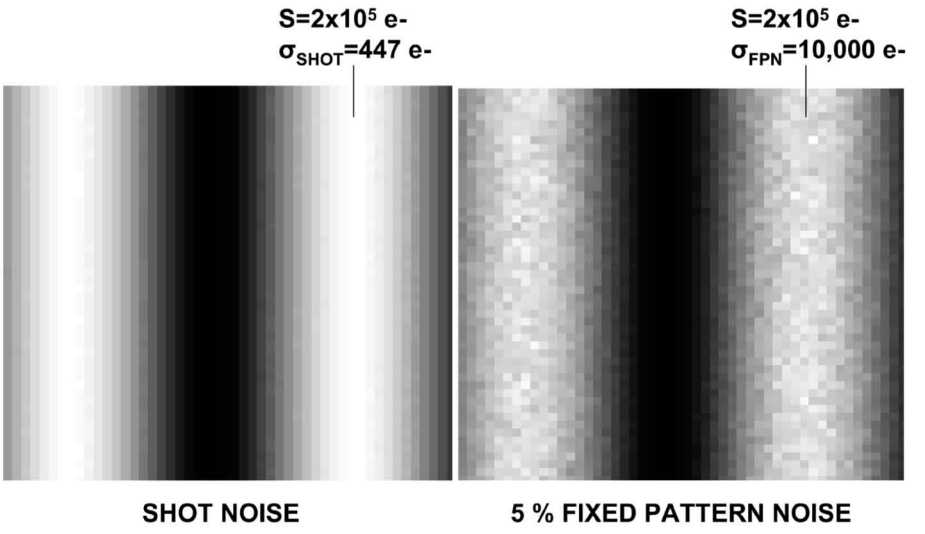

Figure 3.14 Sinusoidal images with and without FPN at the same average signal level.

FPN and shot noise can be compared by their ratio [i.e., Eqs. (3.12) and (3.6)] as

$$\frac{\sigma_{\mathrm{FPN}}}{\sigma_{\mathrm{SHOT}}} = P_{\mathrm{N}}\left(\frac{S}{\eta_{\mathrm{i}}}\right)^{1/2}. \tag{3.13}$$

Figure 3.15 plots this ratio as a function of signal and quantum yield.

The signal level where FPN equals signal shot noise is found by setting Eq. (3.13) to unity and solving for signal to produce

$$S_{\mathrm{SHOT=FPN}} = \frac{\eta_{\mathrm{i}}}{P_{\mathrm{N}}^2}; \tag{3.14}$$

or, in terms of photon energy,

$$S_{\mathrm{SHOT=FPN}} = \frac{h_\nu}{3.65P_{\mathrm{N}}^2}. \tag{3.15}$$

Example 3.6

Determine the signal level when $\sigma_{\mathrm{FPN}} = \sigma_{\mathrm{SHOT}}$ for $\eta_{\mathrm{i}} = 1$ and 100. Assume $P_{\mathrm{N}} = 0.01$.

Solution:
From Eq. (3.14),

$$S_{\mathrm{SHOT=FPN}} = \frac{1}{0.01^2} = 10{,}000\ \mathrm{e}^-, \quad \eta_{\mathrm{i}} = 1;$$

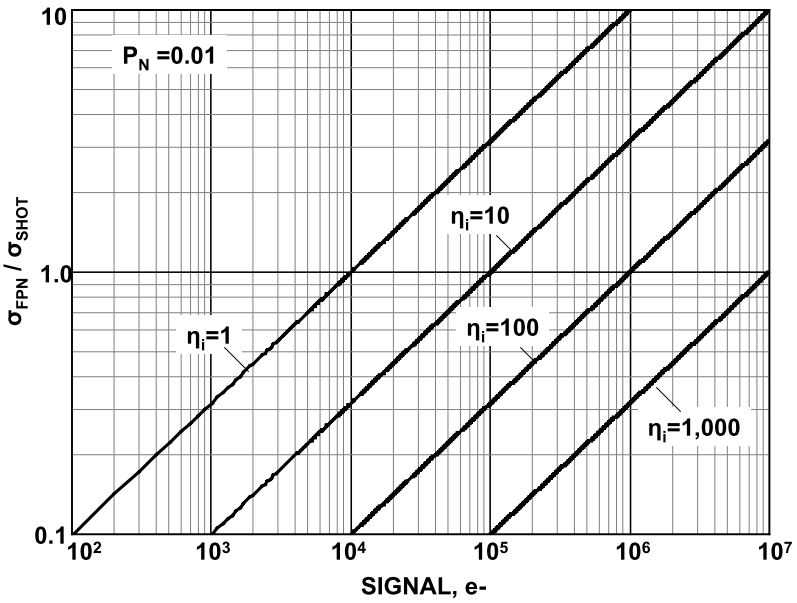

Figure 3.15 FPN/shot noise ratio as a function of signal at different quantum yields.

and

$$S_{\mathrm{SHOT=FPN}} = \frac{100}{0.01^2} = 10^6 \text{ e}^-, \quad \eta_{\mathrm{i}} = 100.$$

These results are also shown in Fig. 3.15.

Most CMOS and CCD detectors do not exhibit a charge capacity as large as 10^6 e^-. Therefore, x-ray sensors will be dominated by signal shot noise instead of FPN common to visible detectors (also refer to Fig. 10.3).

As mentioned above, the minimum FPN for CCD and CMOS imagers is approximately 1% of the signal level. Many other FPN sources contribute to a measurement increase of P_{N} above the ideal. For example, dust particles situated above pixels block the incoming light and generate additional FPN. A few particulates within a region of interest can have a dramatic effect on PT statistics. When FPN noise is limited by this problem, P_{N} represents a measurement of device cleanliness and not the detector itself. Optical effects such as vignetting, shading, and interference fringing also fall into the category of FPN sources. For example, Fig. 3.16 shows a 5461 A flat-field image with deep fringes generated by a CCD. The interference pattern is caused by light reflections between the sensor's surface and the optical window, which are nearly perfectly flat to one another. This image exhibits a FPN of approximately 10%—10 times greater than the ideal pixel-to-pixel FPN nonuniformity. Fortunately, all FPN sources can be readily removed through the process of flat fielding (see Chapter 8).

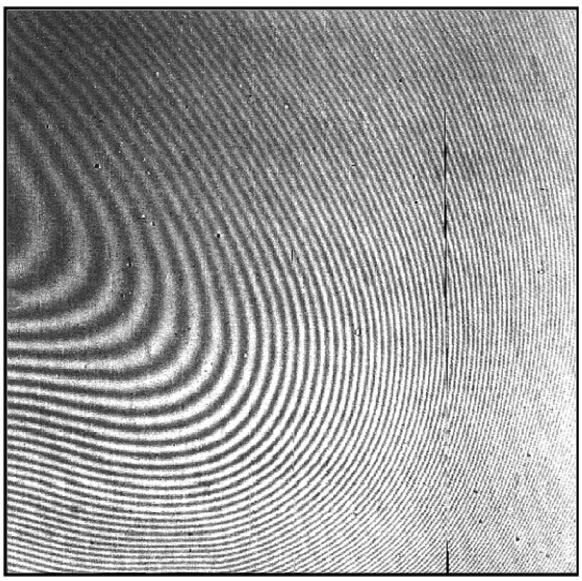

Figure 3.16 Optical interference fringes and dust spots resulting in high FPN.

3.5 Read Noise

Chapter 11 is devoted to important read noise sources encountered in CCD and CMOS imagers and camera systems. *Read noise* is defined as any noise source that is not a function of signal.

Shot noise, FPN, and Fano noise can be added in quadrature with read noise to produce the total noise equation,

$$\sigma_{\mathrm{TOTAL}} = (\sigma^2_{\mathrm{READ}} + \sigma^2_{\mathrm{FN}} + \sigma^2_{\mathrm{SHOT}} + \sigma^2_{\mathrm{FPN}})^{1/2}; \tag{3.16}$$

or, equivalently,

$$\sigma_{\mathrm{TOTAL}} = (\sigma^2_{\mathrm{READ}} + \eta_{\mathrm{i}} F_{\mathrm{F}} + \eta_{\mathrm{i}} S + (P_{\mathrm{N}} S)^2)^{1/2}, \tag{3.17}$$

where σ_{TOTAL} is the total noise (e^- rms), and σ_{READ} is the read noise (rms e^-). The four noise sources are Gaussian distributed. The PTCs generated in Chapter 5 plot each noise source separately as a function of signal.

Important Points

1. Shot and Fano noise are fundamentally related to the charge generated by a photon's interaction with a semiconductor.
2. Shot noise increases by the square root of the signal and quantum yield, whereas Fano noise increases by the square root of the quantum yield.
3. Fano noise is observed in PTCs when the number of interacting photons is less than the number of pixels.
4. FPN is associated with pixel-to-pixel sensitivity differences that increase directly with signal.
5. The minimum FPN noise achieved by CCD and CMOS imagers is approximately 1% of the signal level.
6. For wavelengths > 4000 A, FPN begins to dominate shot noise at a signal level of approximately 10,000 e^- (i.e., $1/P^2_{\mathrm{N}}$). For wavelengths < 4000 A, shot noise increases relative to FPN by the quantum yield gain.
7. Read noise encompasses all noise sources that are signal independent.